

Quorum Quenching Nanofibers for Anti-Biofouling Applications

Amos Taiswa ^{1,2,*}, Jessica M. Andriolo ^{1,2} , M. Katie Hailer ³ and Jack L. Skinner ^{1,2}

¹ Montana Tech Nanotechnology Laboratory, Montana Technological University, Butte, MT 59701, USA; jandriolo@mtech.edu (J.M.A.); jskinner@mtech.edu (J.L.S.)

² Department of Mechanical Engineering, Montana Technological University, Butte, MT 59701, USA

³ Department of Chemistry and Geochemistry, Montana Technological University, Butte, MT 59701, USA; khailer@mtech.edu

* Correspondence: ataiswa@mtech.edu

Abstract: Biofilms, complex microbial communities, adept at forming on diverse surfaces within environments, such as membrane technologies, ship hulls, medical devices, and clinical infections, pose persistent challenges. While various biofilm prevention methods, including antimicrobial coatings, physical barriers, and bacteriophage utilization, have been devised for engineered systems, their efficacy fluctuates based on application type and microbial species. Consequently, there remains a pressing need for the development of highly targeted and efficient biofilm control strategies tailored to specific applications remains a pressing need. In our investigation, we disrupt microbial cell-to-cell communication in *Pseudomonas aeruginosa* through the application of anti-quorum sensing (anti-QS) furanone C-30 molecules. The incorporation of these molecules onto electrospun surfaces yielded substantial reductions of 69% in petri dish assays and 58% on mixed cellulose ester (MCE) membranes in a dead-end nanofiltration system, showcasing the potent anti-biofouling impact. Notably, the functionalization of MCE surfaces with anti-QS molecules resulted in a remarkable 16.7% improvement in filtration output. These findings underscore the potential of this targeted approach to mitigate biofilm formation, offering a technical foundation for advancing tailored strategies in the ongoing pursuit of effective and application-specific biofilm control measures.

Keywords: quorum sensing; biofilms; electrospinning; anti-biofouling; nanotechnology; filtration



Citation: Taiswa, A.; Andriolo, J.M.; Hailer, M.K.; Skinner, J.L. Quorum Quenching Nanofibers for Anti-Biofouling Applications. *Coatings* **2024**, *14*, 70. <https://doi.org/10.3390/coatings14010070>

Academic Editor: Paul Balaure

Received: 14 November 2023

Revised: 16 December 2023

Accepted: 2 January 2024

Published: 4 January 2024



Copyright: © 2024 by the authors. Licensee MDPI, Basel, Switzerland. This article is an open access article distributed under the terms and conditions of the Creative Commons Attribution (CC BY) license (<https://creativecommons.org/licenses/by/4.0/>).

1. Introduction

Biofouling is a common source of failure for implanted medical devices, nautical equipment, and membrane-based water treatment processes [1–3]. Biofouling involves the excessive growth and proliferation of microorganisms that result in biofilm formation on these devices, ultimately damaging output or performance. Biofilms consist of organic compounds, such as carboxylic and amino acids, proteins, and carbohydrates, and they are made of protective architectures that provide a safe environment for potentially harmful organisms to thrive. These protective architectures are made up of extracellular polymeric substances (EPSs) that are released by microorganisms and cover the majority of biofilms to protect against biocides [4,5]. Severe medical complications can arise from biofilm formation because these complex, shielding ecosystems can render drug interventions less effective or completely ineffective [6]. Increased drag on U.S. naval ships due to biofouling has resulted in a cost of ~USD 2.1 billion annually [7,8]. Biofilms are also an issue in pressure-driven water systems, where the films grow on filtration membranes, resulting in decreased water output and membrane life [9]. Currently, a wide array of fundamental studies on biofilms and biofouling prevention are being performed to mitigate the issues caused by biofilm formation on engineered systems. However, the issue is far from being eradicated, and solutions proposed provide new concerns. For instance, the use of biocides, such as copper, silver, and tributyltin, has triggered environmental and human health concerns due to their toxicity [10,11]. In some cases, the use of biocides

necessitates the need for treatment and/or recovery from the brine system, which can be cost prohibitive [12]. Other solutions proposed involve the modification of surfaces to provide a physical deterrent for the adherence of one species. While this solution minimizes toxicity concerns, results show that surface modifications may prevent microorganismal adherence in one species while encouraging adherence in the next [10,13].

Membrane biofouling remains a critical challenge in various membrane-based separation processes, such as reverse osmosis, ultrafiltration, and microfiltration. The accumulation of unwanted biological substances, including bacteria, algae, and organic matter, on the membrane surface leads to reduced flux, increased energy consumption, and compromised long-term performance [9]. Recent studies have highlighted the intricate interplay between microbial adhesion, biofilm formation, and the physicochemical properties of membranes and other surfaces [14]. Understanding these interactions is essential for developing effective biofouling mitigation strategies. Researchers have explored novel materials with anti-fouling properties, such as zwitterionic polymers and graphene oxide, to modify membrane surfaces and discourage biofilm formation [15,16]. Additionally, advancements in bio-inspired design, including biomimetic coatings and surface modifications inspired by natural anti-fouling mechanisms, show promise in enhancing the resistance of membranes to biofouling [17].

To address membrane biofouling, recent efforts have also focused on the development of innovative cleaning and fouling control techniques. In situ monitoring and control strategies, such as the use of advanced sensors and artificial intelligence algorithms, enable real-time detection of fouling events and adaptive responses [18]. Furthermore, sustainable approaches, including the use of enzymes or environmentally friendly bio-based agents [19], have gained attention as alternatives to traditional chemical cleaning methods. Integrating these multifaceted approaches into a holistic framework offers a promising avenue for mitigating membrane biofouling and improving the efficiency and longevity of membrane-based separation processes. Sustainable approaches to mitigate membrane biofouling have witnessed a notable surge of interest in the recent literature, with a particular focus on quorum-sensing (QS) molecules [20–22]. Quorum sensing, a cell-to-cell communication mechanism among microorganisms, plays a pivotal role in the regulation of biofilm formation. Researchers are exploring the use of quorum-sensing inhibitors as a novel strategy to disrupt the communication signals that orchestrate biofilm development on membrane surfaces [9]. By targeting the microbial communication pathways, these inhibitors can potentially hinder the initial stages of biofilm formation, thereby reducing the propensity for membrane fouling [20]. This sustainable approach offers the advantage of specificity, as it disrupts biofilm formation without resorting to conventional chemical biocides, thereby minimizing the environmental impact. As investigations in this field progress, the integration of quorum-sensing inhibition into membrane design and operation could represent a promising avenue for sustainable biofouling control in membrane-based separation processes.

In this work, an electrospun fiber coating for filtration membranes was used to provide disruptive texture and slow release of molecules that interrupt bacterial signaling. QS is used by bacteria to release signaling molecules in response to changing bacterial concentrations [23]. QS plays an early and vital role in biofilm formation [24] and, therefore, we hypothesized that disruption of QS signals at the membrane surface would mitigate biofouling. The electrospun coating was fabricated using biocompatible polymer blends containing hydrophilic polyethylene glycol (PEG) and hydrophobic polycaprolactone (PCL) components that provided controlled time release of anti-QS molecules from a nanofiltration membrane to prevent biofilm formation. The performance of the anti-biofouling coatings was evaluated via confocal microscopy and scanning electron microscopy (SEM). Nanofiltration efficiency (water output, flux) was determined using a bench-scale nanofiltration system.

2. Experiment

2.1. Materials

5Z-4-Bromo-5-(bromomethylene)-2(5H)-furanone (Furanone-C30) at a molecular weight of 253.88 g/mol was purchased from Tocris Bioscience (Minneapolis, MN, USA). Curcumin (*Curcuma longa*) was purchased from Sigma Aldrich (St. Louis, MO, USA). The molecules were dissolved in dimethyl sulfoxide (DMSO, Fisher Scientific, Waltham, MA, USA) to obtain desired concentrations in agar plates, petri dish dilution assays, and in the final electrospinning (ES) solutions for the selected molecules. Polycaprolactone (PCL), chloroform and polyethylene glycol (PEG) were purchased from Sigma Aldrich.

2.2. Bacterial Culture

Pseudomonas aeruginosa (PAO1) was purchased from ATCC (47085) and grown in Luria Bertani (LB) broth and agar (Thermo Fisher Scientific, Waltham, MA, USA) for liquid and plated culture, respectively.

2.3. Anti-Quorum-Sensing Activity

An overnight culture of *Pseudomonas aeruginosa* was diluted with sterile, deionized (DI) water to 10^5 cells/mL as determined by a Logos Biosystems LUNA-FL™ dual-fluorescence cell counter and PhotonSlides™. Furanone C-30 was seeded at 5, 50 and 100 µg/mL onto LB agar containing 6 wt. % glucose and left to solidify before spotting the plates with 150 µL of PAO1 at 10^5 cells/mL. Control agar plates were also seeded with PAO1 at 10^5 cells/mL. The plates were incubated for 18 h at 37 °C. Reductions in PAO1 motility diameters were used to determine the anti-QS activity of furanone-C30. Dilute cultures (6 mL) of PAO1 at 10^5 cells/mL were dropped into petri dishes and supplemented with furanone C-30 at 5, 50 and 100 µg/mL. Curcumin was tested in petri dish dilutions at concentrations of 100, 250, 500 and 1000 µg/mL. A petri dish without anti-QS molecules was used as a control. The petri dishes were incubated for 18 h at 37 °C before the biofilm was dyed with biofilm. Volume measurements were performed using a Leica SP8 confocal microscope (CLMS, Leica Microsystems, Deerfield, IL, USA). The experiments were performed in triplicates.

2.4. Electrospinning Parameters

The ES solution was prepared by mixing furanone C-30 in DMSO at selected concentration with 9 wt. % PCL and 3 wt. % PEG in chloroform at 80 °C at constant stirring (360 rpm) for approximately 1 h. ES was performed on a SprayBase® vertical unit equipped with a 22-gauge needle (spinneret). The polymer solution was injected into electrostatic field at 0.25 mL/h. A separation distance of 4 cm was maintained between the spinneret and parallel collector electrodes placed equidistant from the spinneret (parallel gap ES) with an accelerating voltage of 6.6 kV. In this setup, the voltage initiation resulted in fiber deposition swinging back and forth between the two electrodes, resulting in an aligned mat structure. The mat was turned 180° and the process repeated to form a crosshatched fiber mat over 20 min.

2.5. Fiber Stability in Aqueous Environments

The stability and controlled release mechanism of the electrospun fibers in aqueous environments were determined by soaking the fibers in petri dishes containing ultrapure water for 4 h. The anti-QS mechanism of the fibers was determined by placing the fibers in dilute cultures of PAO1 at 10^5 cells/mL for 4 h before imaging biofilm biovolumes on the CLSM. Control fibers were composed of PCL-PEG without furanone C-30.

2.6. Biofouling Simulation and Bench-Scale Testing

The anti-biofouling capabilities of the fibers were investigated on mixed cellulose ester (MCE) nanofiltration membranes using a pressurized bench-scale system (Figure 1). The fibers were electrospun on commercial MCE membranes (25 mm diameter and 50 nm pore size, Millipore, Burlington, MA, USA). Prior to testing, the membrane was sterilized

under ultraviolet light for 15 min in a class II biosafety hood. To better simulate a real-world application, 18 mΩ DI water was used in filtration tests. The DI water was dosed with PAO1 at 10^5 cells/mL and pressurized with a nitrogen tank held at 45 psi. The PAO1-containing water was forced through a filtration cell containing either control or modified MCE membranes. Filtered water was collected in a pre-weighed beaker over 4 h. Experiments were performed in triplicate. Membrane biofouling (biovolume) was quantified by CLSM and SEM.

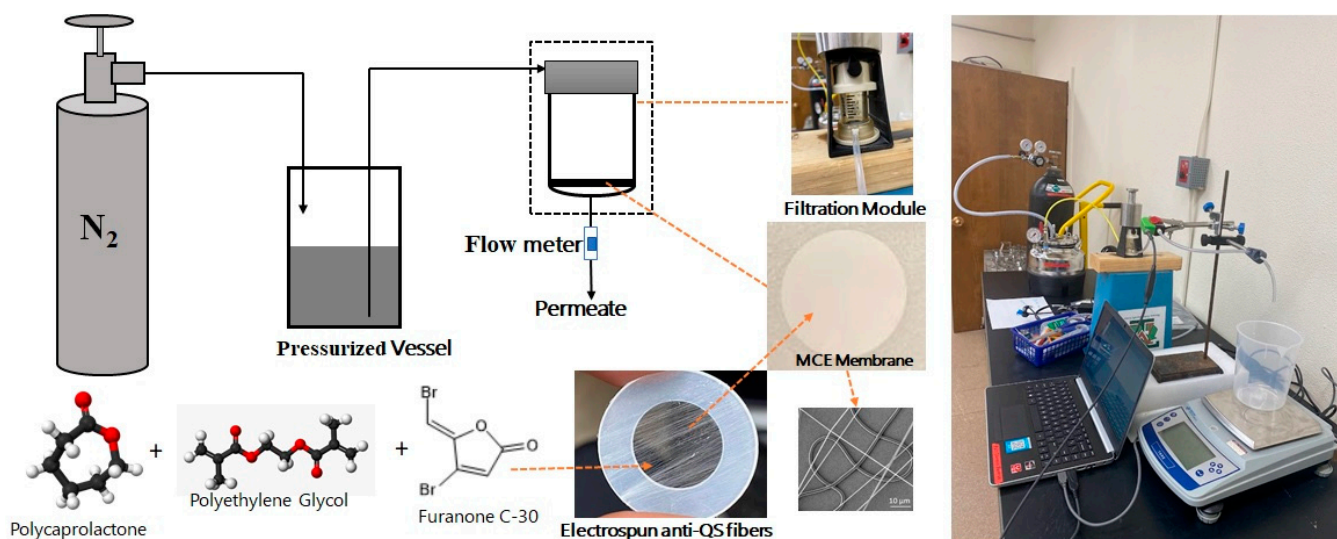


Figure 1. Benchtop nanofiltration system used to monitor water output efficiencies and biofilm formation on MCE nano-filters functionalized with electrospun anti-QS fiber layers.

2.7. Scanning Electron Microscopy

Fiber morphologies were characterized on a Hitachi S-4500 SEM (Hitachi, Tokyo, Japan). A Tescan Mira3 FE-SEM (Tescan, Kohoutovice, Czech Republic) was used to characterize membrane biofilms. Samples were gold coated using a Denton Desk I sputter coater for 60 s at 100 mTorr vacuum and 20 mA.

To prepare the membranes for imaging, the membranes were immediately removed from the benchtop filtration system before being frozen at -80 °C over 2 min. The filters were then gradually dehydrated using an ethanol (EtOH) series of 10, 30, 50, 75, 80, 90 and 100% aqueous EtOH solution. The membranes were then subject to a hexamethyldisilane (HMDS)/EtOH drying series, which included soaking in 3:1 and 1:3 HMDS-to-EtOH solutions. The final sample was dried using 100% HMDS and left overnight in a fume hood prior to analysis.

2.8. Confocal Microscopy

Biofilm biovolumes were characterized using confocal microscopy (CLSM, Leica SP8). A L13152 LIVE/DEAD™ BacLight™ bacterial viability kit (Thermo Fisher Scientific) containing SYTO 9 for live cell staining and Propidium iodide for dead cell staining was used in staining. A water immersion 20× magnification, 0.5 numerical aperture objective lens was used for all experiments. SYTO 9 was excited with an optically pumped semiconductor laser (OPSL) at 488 nm, smart gain maintained at 800 V and Propidium Iodide (PI) excited with an OPSL at 522 nm, smart gain held at 50%. Biofilm z-stacks were taken for each sample. Images were exported as tiff files and biofilms quantified on ImageJ using a COMSTAT2.1 plugin.

3. Results and Discussions

3.1. Antibacterial Action of Furanone C-30 and Curcumin

In Figure 2A–D, the anti-biofouling efficacy resulting from furanone C-30's anti-Quorum-sensing (anti-QS) activity on PAO1 growth is vividly illustrated by the corresponding halo diameters. Notably, Figure 2E reveals a direct correlation between the concentration of furanone C-30 and a discernible reduction in halo diameters on LB agar. At a concentration of 5 $\mu\text{g}/\text{mL}$, treatment with furanone C-30 did not yield a significant difference in halo diameters compared to the control. However, escalating concentrations to 50 $\mu\text{g}/\text{mL}$ and 100 $\mu\text{g}/\text{mL}$ led to a considerable reduction in PAO1 halo diameters by 25% and 48%, respectively. In contrast, Figure 3 demonstrates that curcumin, even at higher concentrations of 1 mg/mL , exhibited no discernible impact on mature PAO1 biofilms. This finding underscores the specificity of furanone C-30 in effectively mitigating PAO1 biofilm growth, highlighting its potential as a targeted anti-biofouling agent. The concentration-dependent response observed in Figure 2E further emphasizes the dose-dependent efficacy of furanone C-30 in impeding the growth of PAO1, substantiating its role as a potent inhibitor of quorum-sensing mechanisms and a promising candidate for biofilm control applications.

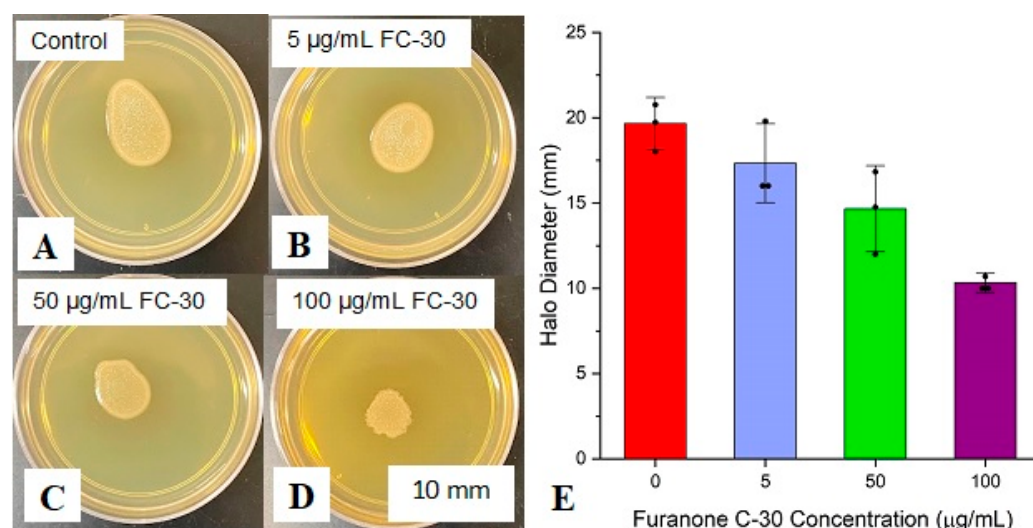


Figure 2. Images showing halo diameters of PAO1 treated with the shown concentration of furanone C-30 (A–D). The effects of furanone C-30 on growth diameters of PAO1 grown for 18 h at 37 °C is shown in part (E).

Visual confirmation of furanone C-30's effectiveness in diminishing biofilm formation was achieved through confocal laser scanning microscopy (CLSM), yielding quantitative insights into alterations in biovolume (Figure 4). Aligning with the concentrations utilized in the halo diameter experiments (0, 5, 50, 100 $\mu\text{g}/\text{mL}$), biovolume studies underscore the concentration-dependent anti-biofouling efficacy of furanone C-30. As illustrated in Figure 4, the efficacy of furanone C-30 exhibits a distinct reliance on concentration. In cultures seeded with a low furanone C-30 concentration (5 $\mu\text{g}/\text{mL}$), the biofilm biovolume and mean thickness experienced reductions of 28.5% and 18.9%, respectively. Escalating the concentration to 50 $\mu\text{g}/\text{mL}$ resulted in a more pronounced reduction, with the biofilm biovolume decreasing by 38.2%, and the mean thicknesses reduced by 27.6%. Impressively, the introduction of furanone C-30 at a concentration of 100 $\mu\text{g}/\text{mL}$ led to a substantial reduction in biofilm biovolume by 97.8%, and decreased mean thicknesses by 98.1% compared to the control. These findings provide quantitative evidence of furanone C-30's robust anti-biofouling activity, reinforcing its potential as a concentration-sensitive inhibitor with significant implications for biofilm control.

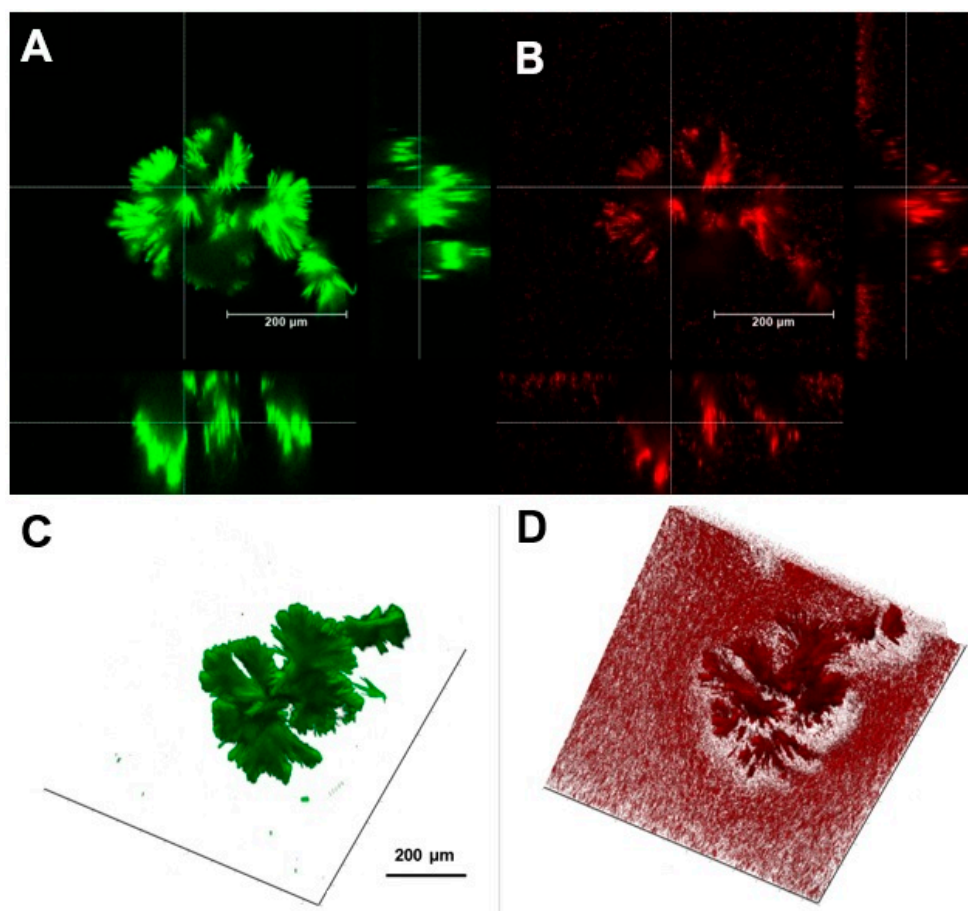


Figure 3. Minimalistic effect of curcumin on mature PAO1 biofilms. (A) Live biofilm of a mature biofilm and (B) dead biomass of PAO1 biofilm with their respective 3D constructions (C) live and (D) dead biomass.

3.2. Controlled Release Mechanism

Using a systematic formulation of multiple polymer blends incorporating PCL-PEG, we aimed to assess their feasibility and establish an optimal controlled release profile. Combining the highly hydrophilic PEG with the hydrophobic PCL created a polymer blend recognized for its success in treatment delivery applications, allowing for the gradual release of therapeutic agents over an extended period [25]. The present investigation successfully leveraged the intrinsic properties of the polymer blend to attain an optimal release profile that would maintain structure over 4 h through systematic manipulation of the polymer weight ratio between PCL and PEG, as depicted in Figure 5A–D. Elevated concentrations of PEG within the fibers led to minimal pore formation, accompanied by pronounced instances of fiber breakage and disintegration (Figure 5B). Conversely, optimizing the PCL content to three-times the weight percentage of PEG preserved the structural integrity of the fibers while concurrently promoting the development of a highly porous fibrous network (Figure 5E,F). The resultant fiber diameters exhibited a range spanning from 1 to 8 μm . To fabricate the anti-biofouling electrospun fibers, furanone C-30 was homogeneously pre-mixed into the polymer blend prior to initiating fiber formation through ES. Upon exposure to an aqueous environment, the resultant fibers exhibited porosity, facilitated by the dissolution of PEG, thereby releasing any encapsulated molecules, as depicted in Figure 5. Extensive research on the release profiles of anti-QS molecules, including furanone C-30 [26] and Curcumin [27], has been conducted. It is theorized that the enduring porous PCL fiber structure retained embedded furanone C-30 within the stable PCL polymer. The synergistic effects of porosity, embedded functionality, and the ultra-high surface area of the fibers collectively contributed to a highly favorable release

profile spanning 4 h, effectively impeding biofilm growth. This intricate interplay between polymer characteristics and furanone C-30 incorporation underscores the efficacy of the designed system, positioning it as a promising candidate for controlled release applications with significant implications for biofilm control.

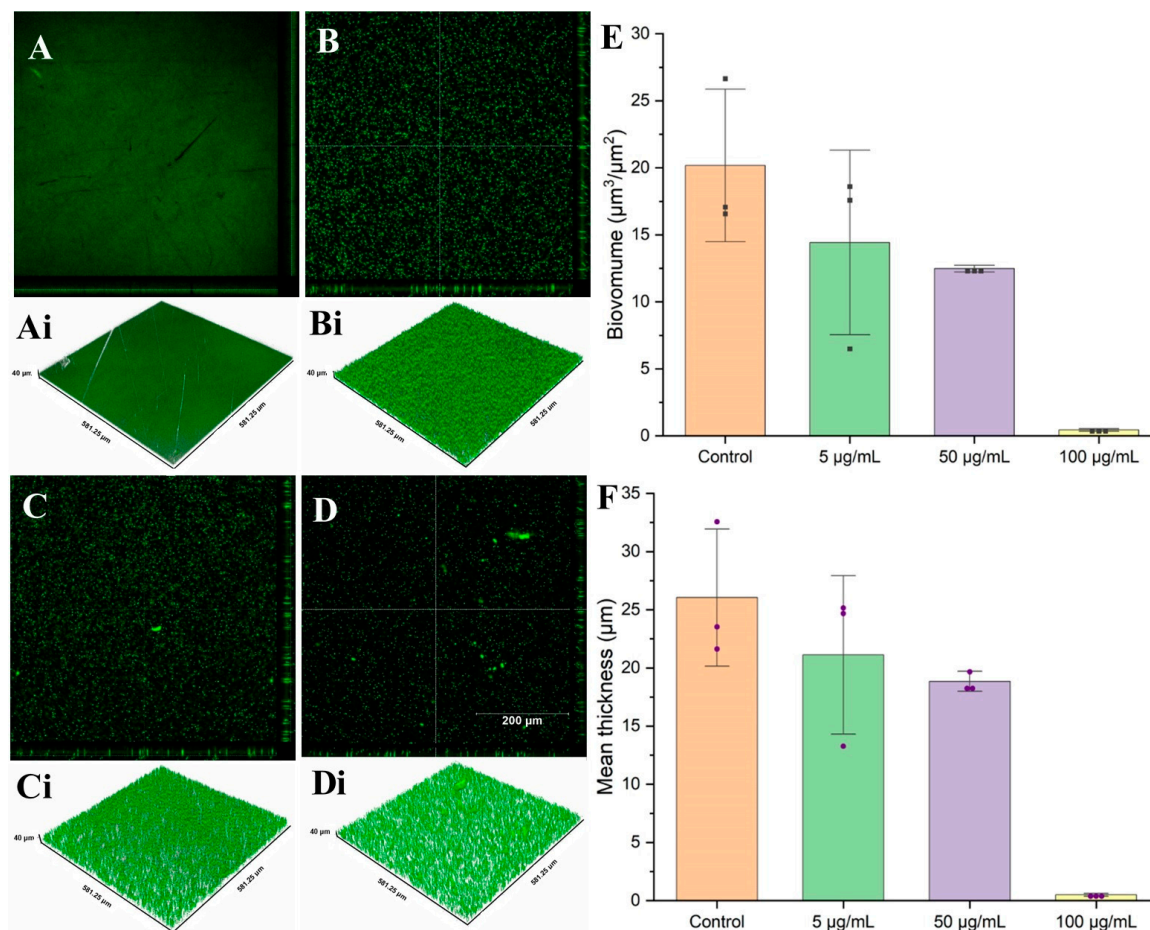


Figure 4. CLSM images of PAO1 biofilm assays of (A) untreated control, (B) 5 µg/mL, (C) 50 µg/mL, and (D) 100 µg/mL furanone C-30 with their respective 3D images (Ai,Bi,Ci,Di), and biovolume (E) and mean thicknesses (F) data summarized from ImageJ plugin COMSTAT2.

The mechanistic release of furanone C-30 from the fibers unfolds through a gradual biofilm growth on the highly porous fibers over a 4 h period. During this phase, as the furanone C-30 molecules dissolve in the aqueous media, the fibers become increasingly susceptible to fouling, as evident in Figure 6, where biofilms engulf the fibers. Conversely, minimal biofilm growth is observed in the aqueous media where furanone C-30 molecules have dissolved (Figure 4). This observation underscores the potential significance of molecule solubility in the sustained effectiveness of anti-biofouling applications. The interplay between the release kinetics and the solubility of furanone C-30 becomes crucial in understanding and optimizing its prolonged efficacy against biofilm formation.

3.3. Anti-QS Performance of Electrospun Surface

The comparison of biofilm growth patterns around mixed cellulose ester (MCE) membranes, featuring electrospun control fibers and those functionalized with furanone C-30, was conducted using *Pseudomonas aeruginosa* (PAO1). Following a 4 h incubation period at room temperature in a stationary setting, the biovolume of the biofilm beneath functionalized fibers measured 5.40 µm³ per µm² of the MCE membrane, representing a substantial 69.02% decrease compared to the biofilm formed under control fibers (7.44 µm³ per µm²). Notably, surfaces equipped with anti-quorum-sensing (anti-QS) fibers demonstrated signifi-

cant mitigation of biofilm formation, in stark contrast to electrospun control surfaces lacking anti-QS molecules, as depicted in Figure 7. These results underscore the remarkable efficacy of the anti-QS-functionalized fibers in impeding biofilm growth around MCE membranes, highlighting their potential as a targeted approach for biofouling control applications.

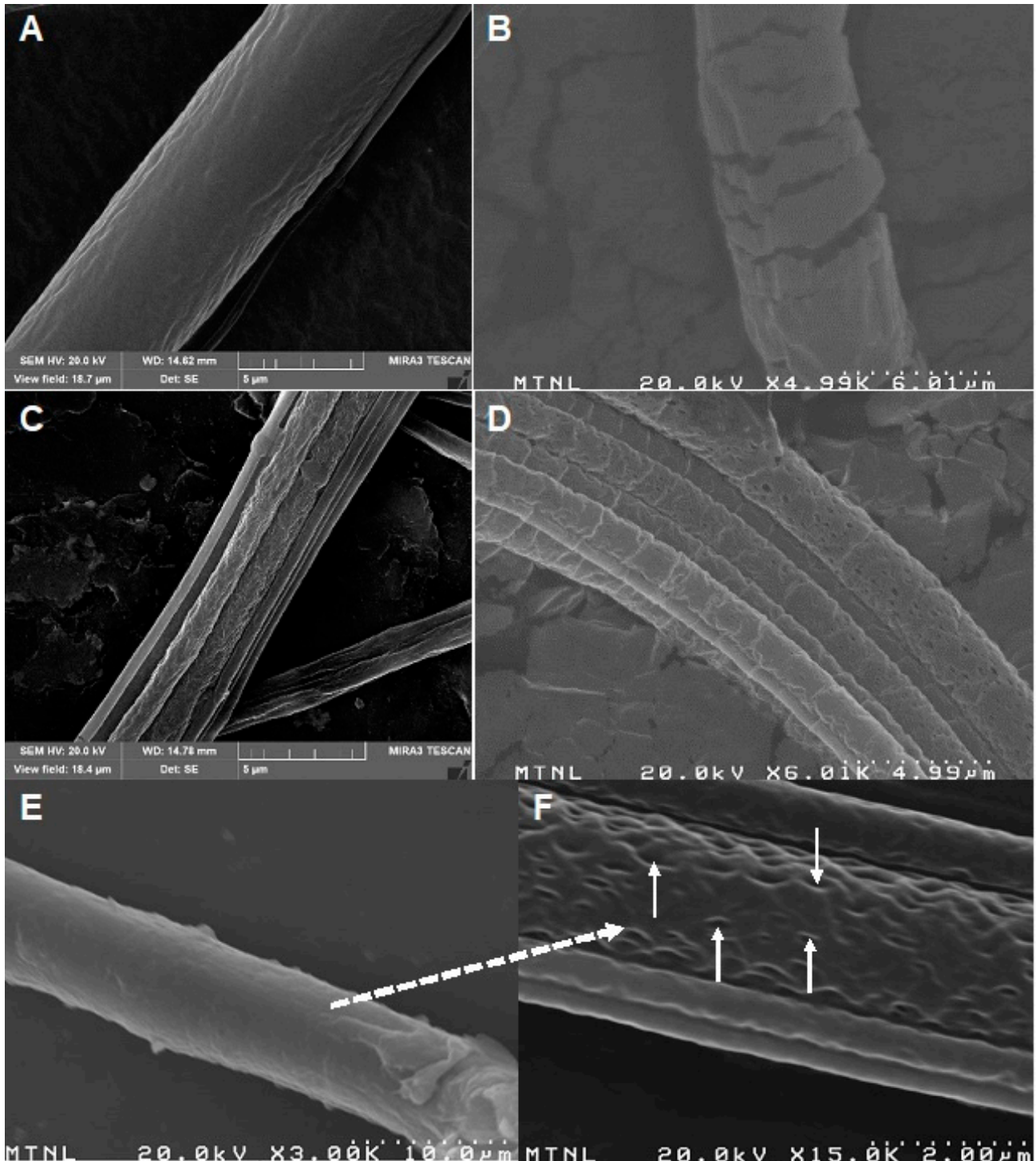


Figure 5. Scanning electron micrograph of (A) A control PCL-PEG fiber pre-exposure to an aqueous media; (B) Elevated concentrations of PEG exposed to DI water (1PEG:1PCL weight ratios); (C) 1PEG:2PCL exposed to DI water; (D) 1PEG:3PCL fibers exposed in aqueous media; (E,F) pore formation process in PCL-PEG fibers following release of furanone C-30 molecules in aqueous solution over 4 h.

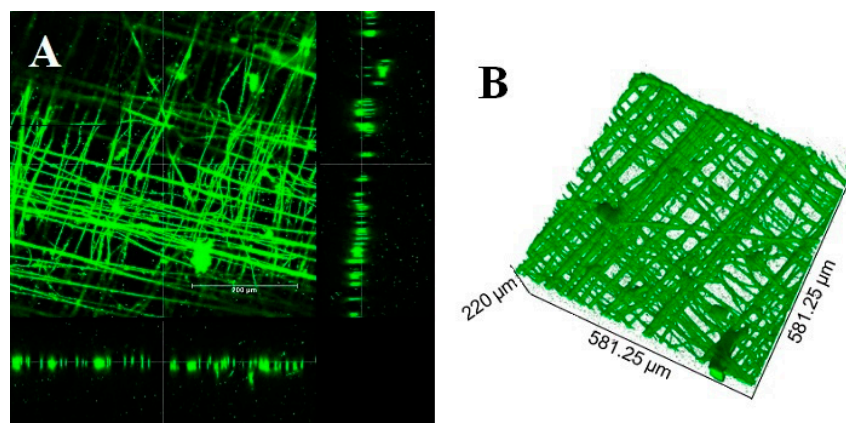


Figure 6. Biofilm formation on electrospun PCL-PEG fibers as furanone C-30 dissolved into solution. (A) 2D biofilm image and (B) 3D PAO1 biofilm confocal of biofilm formation on the fibers after 4 h.

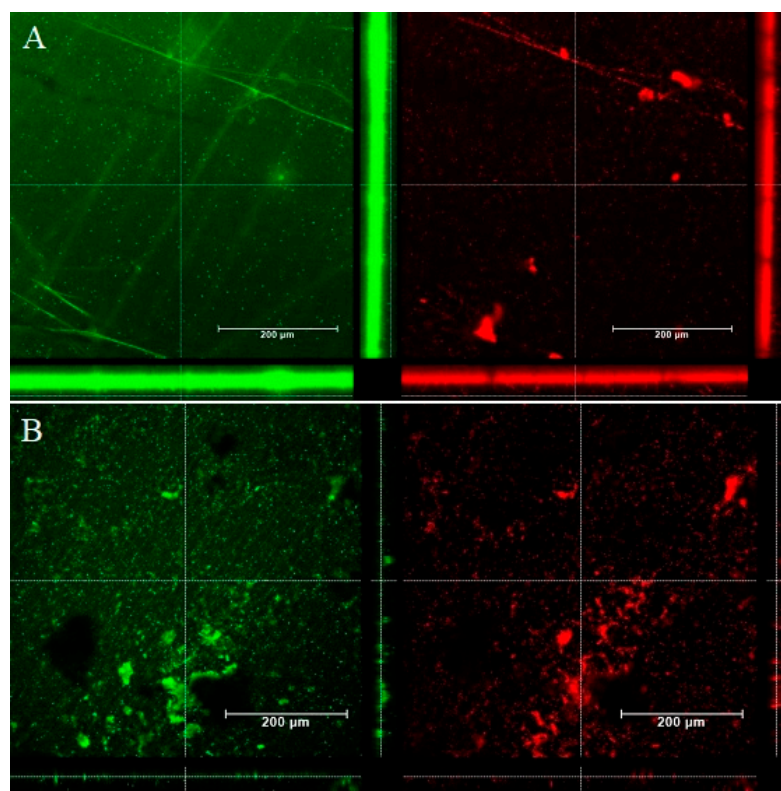


Figure 7. *Pseudomonas aeruginosa* biofilms growth on MCE membranes coated with (A) control PCL-PEG fibers and (B) PCL-PEG fibers functionalized with furanone C-30 molecules in petri dish assays after a 4 h operation. The images with orthogonal cross-sections represent live (green) and dead (red) biofilm signals.

3.4. Nanofiltration Application of the Furanone C-30-Functionalized Membranes

To assess biofouling control and flux performance, a dead-end nanofiltration experiment was conducted, comparing membranes featuring functionalized ES fibers with those having ES PCL-PEG control fibers. Following a 4 h operation, the membranes were removed, and the resulting biofilm structure and biovolume on the membrane surface were visualized using CLSM and SEM. Notably, the biofilm formed on the MCE membrane with control PCL-PEG fibers exhibited a dense and thick structure compared to the significantly mitigated biofilm observed on membranes with anti-QS fibers, as depicted in Figure 8. Quantitative analysis of the PAO1 biovolume, consisting of live cells on the

anti-QS-functionalized MCE membrane surface, revealed a measurement of $16.27 (\pm 8.67) \mu\text{m}^3$ per μm^2 of membrane area. This marked a substantial 57.5% reduction compared to the biovolume on control fibers, which measured $38.26 (\pm 7.55) \mu\text{m}^3$ per μm^2 of membrane area. These findings underscore the pronounced efficacy of anti-QS-functionalized fibers in biofouling control, demonstrating their potential to significantly reduce biofilm formation on membrane surfaces during nanofiltration processes.

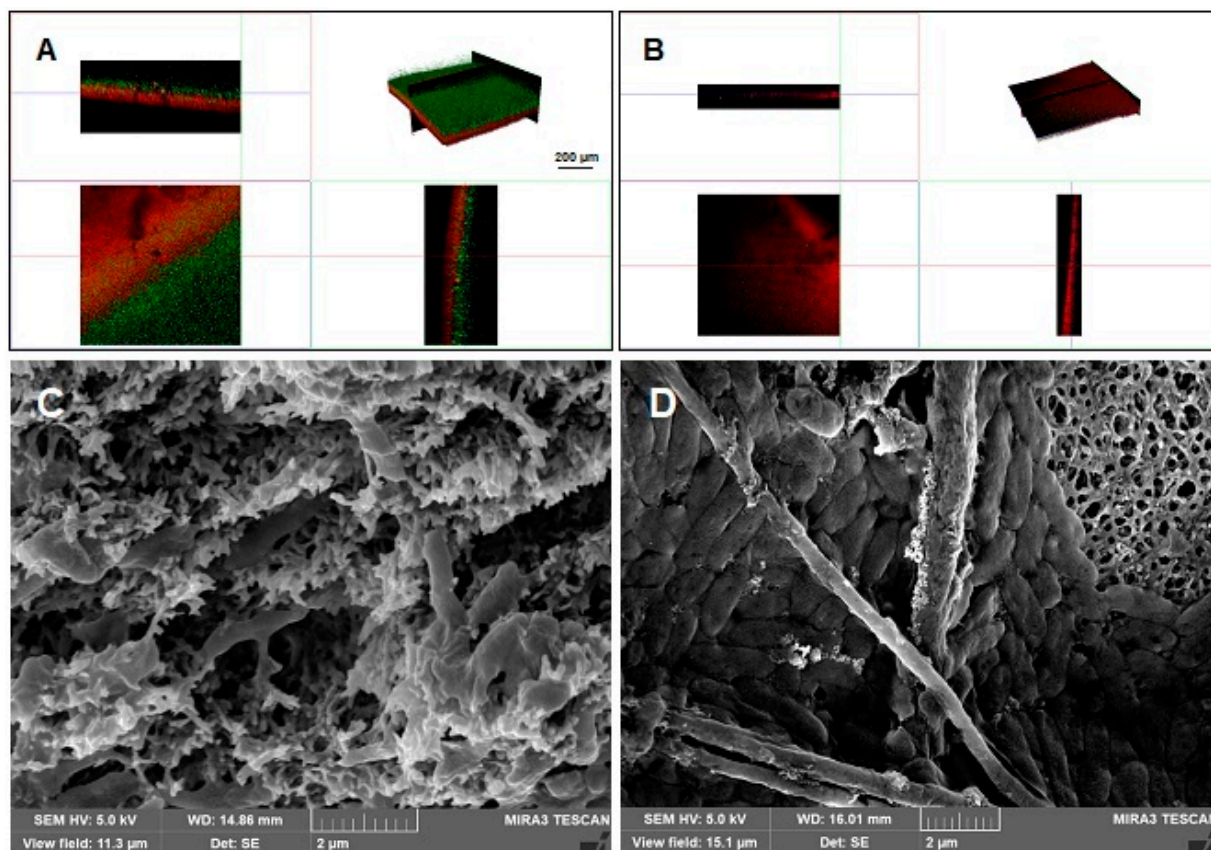


Figure 8. Membrane biofilm after a nanofiltration simulation. (A,C) SEM and confocal micrographs of biofilm formed on the control and (B,D) SEM and confocal micrographs of membrane biofilm in the presence of furanone C-30-functionalized fibers.

To further comprehend the significance of biofouling mitigation in the engineered nanofiltration membrane system, flux was continually monitored and compared between the two membrane surfaces over the 4 h operational period (Figure 9). A slightly higher volume of water was filtered in the presence of anti-QS molecules (180.7 ± 13.8 mL) compared to 150.6 ± 28.6 mL with control PCL-PEG fibers alone, a phenomenon attributable to the presence of an accumulating and expanding microbial community. The normalized flux (J/J_0) decline exhibited similarity for both conditions during the initial half-hour; however, beyond this point, the normalized permeate flux declined more rapidly for PCL-PEG control fibers. Given the hydrophilic nature of furanone C-30 molecules, the authors posit that this property may limit the long-term application of furanone C-30 in open-engineered systems, in contrast to closed systems, as observed in petri dish assays. This observation highlights a critical consideration for the sustained efficacy of furanone C-30 in continuous operational scenarios, emphasizing the need for hydrophobic strategies to address biofouling challenges in practical membrane applications.

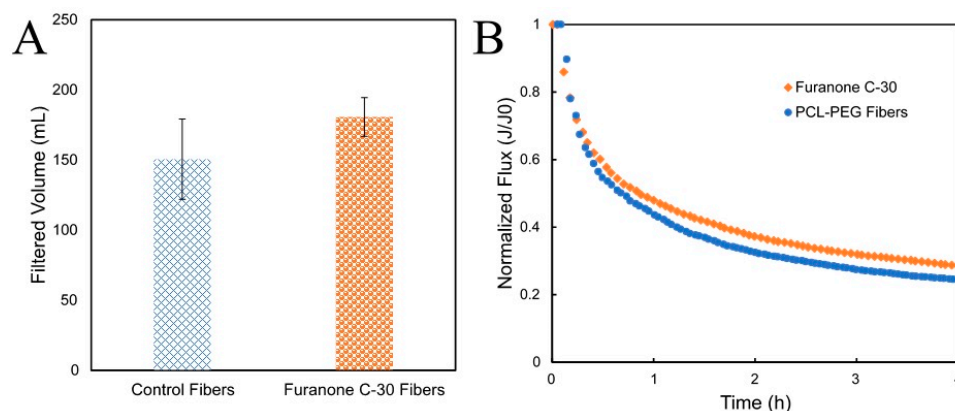


Figure 9. Nanofiltration performance of membranes with control fibers and furanone C-30 fibers. (A) Filtered volume and (B) flux decline over time over 4 h operation.

4. Conclusions

In conclusion, our study showcases the development of a targeted and highly effective biofilm control strategy utilizing anti-quorum-sensing (anti-QS) furanone C-30 molecules to disrupt microbial cell-to-cell communication in *Pseudomonas aeruginosa*. This innovative approach holds significant promise for diverse applications, including membrane technologies, medical devices, and ship hulls, where biofilm formation poses persistent challenges. The introduction of anti-QS molecules on electrospun surfaces demonstrated a remarkable 69% reduction in biofilm growth in petri dish assays, highlighting the potent inhibitory effect on microbial adherence. Importantly, this anti-QS functionalization extended its efficacy to practical applications, with a substantial 58% reduction in biofilm formation observed on MCE membranes within a dead-end nanofiltration system. The tangible impact of this intervention was further emphasized by a notable 16.7% improvement in filtration output when MCE surfaces were equipped with anti-QS molecules. These outcomes underscore the potential of this tailored strategy to enhance the performance and longevity of engineered systems, addressing the critical need for targeted biofilm control measures. The success of this approach not only contributes to the fundamental understanding of biofilm mitigation but also opens avenues for the development of highly specific and application-tailored solutions in the ongoing battle against biofouling challenges.

This observed efficacy underscores the potential of electrospun coatings as a powerful tool in the ongoing efforts to mitigate biofouling challenges. An essential insight derived from this investigation pertains to the critical role of solubility characteristics in influencing the performance of these functionalized surfaces. The careful selection of molecules with specific solubility profiles emerged as a key determinant, shedding light on the nuanced interactions between the anti-QS compounds and the membrane surface. This nuanced understanding contributes to the broader knowledge base on tailored surface engineering, providing crucial insights for optimizing the design of future anti-biofouling coatings. The versatility of this electrospun approach holds promise for widespread application across various engineering domains, ranging from medical devices to water treatment processes. The ability to curb biofilm formation on MCE membranes in a controlled setting underscores the potential for real-world implementation, offering a practical solution to enhance the durability and performance of engineered systems. Overall, this study contributes not only to the fundamental understanding of biofilm mitigation but also provides a tangible and technically sound framework for the development of next-generation anti-biofouling technologies.

Author Contributions: A.T.: Conceptualization, formal analysis, methodology, investigation, writing—original draft. J.M.A.: conceptualization, methodology, formal analysis, writing—original draft. M.K.H.—resources, conceptualization, methodology, writing—original draft. J.L.S.—conceptualization,

methodology, resources, supervision, writing—original draft, funding acquisition. All authors have read and agreed to the published version of the manuscript.

Funding: This material is based upon work supported in part by the National Science Foundation EPSCoR Cooperative Agreement OIA-1757351.

Institutional Review Board Statement: Not applicable.

Informed Consent Statement: Not applicable.

Data Availability Statement: Data are contained within the article.

Acknowledgments: Confocal analysis materials herein are based on work supported by the National Science Foundation under Grant 1828523. Any opinions, findings, and conclusions or recommendations expressed in this material are those of the author(s) and do not necessarily reflect the views of the National Science Foundation.

Conflicts of Interest: The authors have no conflict to disclose.

References

1. Vertes, A.; Hitchins, V.; Phillips, K.S. Analytical challenges of microbial biofilms on medical devices. *Anal. Chem.* **2012**, *84*, 3858–3866. [[CrossRef](#)] [[PubMed](#)]
2. Qiu, H.; Feng, K.; Gapeeva, A.; Meurisch, K.; Kaps, S.; Li, X.; Yu, L.; Mishra, Y.K.; Adelung, R.; Baum, M. Functional polymer materials for modern marine biofouling control. *Prog. Polym. Sci.* **2022**, *127*, 101516. [[CrossRef](#)]
3. Amin, N.A.A.M.; Mokhter, M.A.; Salamun, N.; Mohamad, M.F.; bin Mahmood, W.M.A.W. Anti-fouling electrospun organic and inorganic nanofiber membranes for wastewater treatment. *South Afr. J. Chem. Eng.* **2023**, *44*, 302–317. [[CrossRef](#)]
4. Silva, E.; Ferreira, O.; Ramalho, P.; Azevedo, N.; Bayón, R.; Igartua, A.; Bordado, J.; Calhorda, M. Ecofriendly non-biocide-release coatings for marine biofouling prevention. *Sci. Total Environ.* **2019**, *650*, 2499–2511. [[CrossRef](#)]
5. Jones, I.A.; Joshi, L.T. Biocide use in the antimicrobial era: A review. *Molecules* **2021**, *26*, 2276. [[CrossRef](#)] [[PubMed](#)]
6. Shineh, G.; Mobaraki, M.; Perves Bappy, M.J.; Mills, D.K. Biofilm Formation, and Related Impacts on Healthcare, Food Processing and Packaging, Industrial Manufacturing, Marine Industries, and Sanitation—A Review. *Appl. Microbiol.* **2023**, *3*, 629–665. [[CrossRef](#)]
7. Schultz, M.P.; Bendick, J.A.; Holm, E.R.; Hertel, W.M. Economic impact of biofouling on a naval surface ship. *Biofouling* **2011**, *27*, 87–98. [[CrossRef](#)]
8. Lewis, J.A. Non-silicone biocide-free antifouling solutions. In *Advances in Marine Antifouling Coatings and Technologies*; Elsevier: Amsterdam, The Netherlands, 2009; pp. 709–724. [[CrossRef](#)]
9. Taiswa, A.; Andriolo, J.M.; Katie Hailer, M.; Skinner, J.L. Electrospun controlled release anti-quorum sensing filter for biofouling prevention in MCE membranes. *Sep. Purif. Technol.* **2024**, *332*, 125874. [[CrossRef](#)]
10. Nwuzor, I.C.; Idumah, C.I.; Nwanonyi, S.C.; Ezeani, O.E. Emerging trends in self-polishing anti-fouling coatings for marine environment. *Saf. Extrem. Environ.* **2021**, *3*, 9–25. [[CrossRef](#)]
11. Amara, I.; Miled, W.; Ben Slama, R.; Ladhari, N. Antifouling processes and toxicity effects of antifouling paints on marine environment. A review. *Environ. Toxicol. Pharmacol.* **2018**, *57*, 115–130. [[CrossRef](#)]
12. Taiswa, A.; Andriolo, J.M.; Zodrow, K.R.; Skinner, J.L. Polydopamine-copper spacers improve longevity and prevent biofouling in reverse osmosis. *Water Supply* **2022**, *22*, 7782–7793. [[CrossRef](#)]
13. Viju, N.; Anitha, A.; Vini, S.S.; Shankar, C.V.; Satheesh, S.; Punitha, S. Antibiofilm activities of extracellular polymeric substances produced by bacterial symbionts of seaweeds. *Indian J. Geo-Mar. Sci.* **2014**, *43*, 2136–2146.
14. Achinas, S.; Charalampogiannis, N.; Euverink, G.J.W. A Brief Recap of Microbial Adhesion and Biofilms. *Appl. Sci.* **2019**, *9*, 2801. [[CrossRef](#)]
15. Ashfaq, M.Y.; Al-Ghouti, M.A.; Zouari, N. Investigating the effect of polymer-modified graphene oxide coating on RO membrane fouling. *J. Water Process. Eng.* **2022**, *49*, 103164. [[CrossRef](#)]
16. Chen, H.; Xu, C.; Zhao, F.; Geng, C.; Liu, Y.; Zhang, J.; Kang, Q.; Li, Z. Designing the anti-biofouling surface of an ultrafiltration membrane with a novel zwitterionic poly(aryl ether oxadiazole) containing benzimidazole. *Appl. Surf. Sci.* **2023**, *609*, 155447. [[CrossRef](#)]
17. Zhang, N.; Cheng, K.; Zhang, J.; Li, N.; Yang, X.; Wang, Z. A dual-biomimetic strategy to construct zwitterionic anti-fouling membrane with superior emulsion separation performance. *J. Memb. Sci.* **2022**, *660*, 120829. [[CrossRef](#)]
18. Jeong, S.; Kim, H.-W. In situ real-time monitoring technologies for fouling detection in membrane processes. In *Current Developments in Biotechnology and Bioengineering*; Elsevier: Amsterdam, The Netherlands, 2023; pp. 43–64. [[CrossRef](#)]
19. Kim, D.Y.; Kim, M.; Jeon, S.; Lee, J.; Park, H.; Park, Y.-I.; Park, S.-J.; Lee, J.-H. In situ modification of ultrafiltration membranes with eco-friendly pyrogallol/taurine to enhance antifouling performance. *J. Memb. Sci.* **2023**, *688*, 122114. [[CrossRef](#)]
20. Feng, Y.; Liang, J.; Liu, X.; Gao, K.; Zhang, Y.; Li, A.; Chen, C.; Hou, L.-A.; Yang, Y. Graphene oxide/methyl anthranilate modified anti-biofouling membrane possesses dual functions of anti-adhesion and quorum quenching. *J. Memb. Sci.* **2023**, *668*, 121265. [[CrossRef](#)]

21. Wang, R.; An, Z.; Fan, L.; Zhou, Y.; Su, X.; Zhu, J.; Zhang, Q.; Chen, C.; Lin, H.; Sun, F. Effect of quorum quenching on biofouling control and microbial community in membrane bioreactors by *Brucella* sp. ZJ1. *J. Environ. Manag.* **2023**, *339*, 117961. [[CrossRef](#)]
22. Zhang, X.; Ma, B.; Zhang, N.; Zhang, H.; Ma, Y.; Song, Y.; Zhang, H. Regulating performance of CANON process via adding external quorum sensing signal molecules in membrane bioreactor. *Bioresour. Technol.* **2023**, *369*, 128465. [[CrossRef](#)]
23. González, J.E.; Keshavan, N.D. Messing with Bacterial Quorum Sensing. *Microbiol. Mol. Biol. Rev.* **2006**, *70*, 859–875. [[CrossRef](#)] [[PubMed](#)]
24. Miller, M.B.; Bassler, B.L. Quorum Sensing in Bacteria. *Annu. Rev. Microbiol.* **2001**, *55*, 165–199. [[CrossRef](#)] [[PubMed](#)]
25. Andriolo, J.M.; Sutton, N.J.; Murphy, J.P.; Huston, L.G.; Kooistra-Manning, E.A.; West, R.F.; Pedulla, M.L.; Hailer, M.K.; Skinner, J.L. Electrospun Fibers for Controlled Release of Nanoparticle-Assisted Phage Therapy Treatment of Topical Wounds. *MRS Adv.* **2018**, *3*, 3019–3025. [[CrossRef](#)]
26. Proctor, C.R.; Taggart, M.G.; O'Hagan, B.M.; McCarron, P.A.; McCarthy, R.R.; Ternan, N.G. Furanone loaded aerogels are effective antibiofilm therapeutics in a model of chronic *Pseudomonas aeruginosa* wound infection. *Biofilm* **2023**, *5*, 100128. [[CrossRef](#)]
27. Wei, J.; Zhang, X.; Zhang, Z.; Ding, X.; Li, Y.; Zhang, Y.; Jiang, X.; Zhang, H.; Lai, H.; Shi, J. Switch-on mode of bioenergetic channels regulated by curcumin-loaded 3D composite scaffold to steer bone regeneration. *Chem. Eng. J.* **2023**, *452*, 139165. [[CrossRef](#)]

Disclaimer/Publisher's Note: The statements, opinions and data contained in all publications are solely those of the individual author(s) and contributor(s) and not of MDPI and/or the editor(s). MDPI and/or the editor(s) disclaim responsibility for any injury to people or property resulting from any ideas, methods, instructions or products referred to in the content.